At the crossroads of astrophysics and cosmology: Period–luminosity relations in the 2020s
Proceedings IAU Symposium No. 376, 2024
R. de Grijs, P. A. Whitelock & M. Catelan, eds.
doi:10.1017/S1743921323002673

Empirical constraints for the instability strip from the analysis of LMC Cepheids

F. Espinoza-Arancibia and B. Pilecki

Nicolaus Copernicus Astronomical Center, Polish Academy of Sciences, Bartycka 18, 00-716 Warsaw, Poland. email: fespinoza@camk.edu.pl

Abstract. The instability strip (IS) of classical Cepheids has been extensively studied theoretically. Comparison of the theoretical IS edges with those obtained empirically, using the most recent Cepheids catalogs available, can provide us with insights into the physical processes that determine the position of the IS boundaries. We investigate the empirical positions of the IS of the classical Cepheids in the Large Magellanic Cloud (LMC) using data of classical fundamental-mode and first-overtone LMC Cepheids from the OGLE-IV variable star catalog, together with a recent high-resolution reddening map from the literature. We studied their position on the Hertzsprung-Russell diagram and determined the IS borders by tracing the edges of the color distribution along the strip. We obtain the blue and red edges of the IS in V- and I-photometric bands, in addition to $\log T_{\rm eff}$ and $\log L_{\odot}$. The results obtained show a break located at the Cepheids' period of about 3 days, which was not reported before. This phenomenon is most likely explained by the depopulation of second and third crossing classical Cepheids in the faint part of the IS, since blue loops of evolutionary tracks in this mass range do not extend blueward enough to cross the IS at the LMC metallicity. Furthermore, our empirical borders show good agreement with theoretical ones published in the literature. This proves that our empirical IS is a useful tool to put constraints on theoretical models.

Keywords. Stars: variables: Cepheids – Stars: evolution – Magellanic Clouds

1. Introduction

During their evolution, intermediate- and high-mass stars can radially pulsate as Classical Cepheids (hereafter Cepheids) when they cross a defined region in the Hertzsprung-Russel diagram (HRD), called the instability strip (IS). Cepheids span a typical mass range between 3 and 13 $M_{\odot}$ (see, e.g. Bono et al. 2000b; Anderson et al. 2016), though Cepheids with masses higher than 13 $M_{\odot}$ are also known (Musella 2022, and references therein). Such stars first cross the IS during the H-shell burning phase, after they leave the main sequence (MS). Later, the star crosses the IS again during the helium-core burning phase, called the blue loop. The time scale of the first crossing is more than 10 times shorter than that of subsequent crossings. Thus, it is assumed that most of the observed Cepheids are burning helium during the second or third crossing of the IS.

The IS has shown not to be really a "strip" but rather to have a "wedge" structure. The structure of the IS was reported originally using Galactic Cepheids by Pel & Lub (1978) and Fernie (1990), while in the Magellanic Clouds it was noted by Martin et al. (1979), and Caldwell & Laney (1991). A large number of theoretical studies have addressed this issue, among them Bono et al. (2000a) showed how nonlinear theoretical models that consider the coupling between pulsation and convection produce an IS much less steep than linear models. Fiorentino et al. (2002), and more recently De Somma et al. (2022),

concluded that the IS location depends on both the metallicity and helium abundance, moving to lower effective temperatures as the metal content increases. Petroni et al. (2003) studied the effect of using different equations of state on the IS topology, finding a weak dependence. Fiorentino et al. (2007) explored the effects of varying the mixing-length parameter l/H_P, finding that the IS becomes narrower as l/H_P increases, these results agree with the recent work done by De Somma et al. (2022). Anderson et al. (2016) conducted a study of the effects of rotation on Cepheid models, finding that the blue edge of the IS does not depend significantly on rotation, while the red edge is affected by metallicity and rotation.

On the other hand, empirical studies have been conducted to study the properties of the IS. Turner (2001) mapped the IS with a sample of 293 Cepheids in the Milky Way with reddening measurements, finding agreement with the results of Pel & Lub (1978), but disagreement with those presented by Fernie (1990). Tammann et al. (2003) obtained period-color and period-luminosity (P-L) relations of a sample of 321 Galactic Cepheids, in addition to 314 and 486 Cepheids from the Large Magellanic Cloud (LMC) and the Small Magellanic Cloud (SMC), respectively. Using these relations, they obtained the IS of the Galaxy and the Magellanic Clouds, finding differences in the slopes of the ISs between the three galaxies. Sandage et al. (2004, 2009) presented a detailed analysis of the samples of 593 and 460 Cepheids from the LMC and SMC, respectively. For both, they found breaks in the P-L relations, as well as in the IS edges. Recently, Narloch et al. (2019) used a sample of over 3200 LMC Cepheids to obtain an empirical IS using a step-detection technique, to find candidates for non-pulsating stars lying inside the IS.

Remarkably, the Optical Gravitational Lensing Experiment (OGLE) project presented an almost complete census of Cepheids in the Magellanic Clouds (Soszyński et al. 2015). In addition, numerous reddening maps have been published in the literature (see, e.g. Inno et al. 2016; Górski et al. 2020; Skowron et al. 2021; Chen et al. 2022). In this context, we aim to obtain an empirical intrinsic IS for the Cepheids in the LMC using the most recent Cepheids catalogs available. The comparison of theoretical IS edges with those obtained empirically can provide us with insights into the physical processes that determine the position of the IS boundaries. For this purpose, we use data of classical fundamental-mode (F) and first-overtone (1O) LMC Cepheids from the OGLE variable star catalog, together with recent high-resolution reddening maps from the literature. We study the position of the Cepheids on the color-magnitude diagram (CMD) and determine the IS borders by tracing their color distribution along the strip. In addition, we compare our empirical borders with theoretical ones presented in the literature.

The outline of this paper is as follows: Sect. 2 describes the sample selection procedure; Sect. 3 describes the method used to obtain the IS borders; Sect. 4 presents a discussion of our results, including a comparison theoretical ISs published in the literature. Finally, Sect. 5 presents our conclusions.

2. Sample selection

We use data of F and 1O Cepheids in the LMC from the OGLE-IV variable stars catalog (Soszyński et al. 2015) and OGLE-III Shallow Survey (Ulaczyk et al. 2013). The data is affected by reddening, produced by the interstellar extinction along the line of sight. To correct for this effect we use the high-resolution (1.7 arcmin × 1.7 arcmin) reddening map of Skowron et al. (2021), which is based on red clump stars from the Magellanic Clouds, selected from the OGLE-IV catalog. This map has shown good agreement with previous and other recent reddening maps (e.g. Inno et al. 2016; Chen et al. 2022), and yields a small dispersion compared to other maps in the literature. This last feature is important when trying to recover the intrinsic IS, as discussed in Sect. 3.

https://doi.org/10.1017/S1743921323002673 Published online by Cambridge University Press

In order to clean our sample, we discarded 164 objects deviating more than 3 sigma from the reddening-free period-luminosity relationship (also known as period-Wesenheit or P-W relation). A significant fraction of them are objects located significantly above the period-luminosity (P-L) relationship, which were identified recently to be mostly binary Cepheids with giant companions (Pilecki et al. 2021, 2022; Pilecki 2022). Moreover, we discarded 112 Cepheids that presented remarks in the OGLE-IV catalog, to avoid objects that have uncertain characterization. In addition, following the method described in Madore et al. (2017), 113 Cepheids were not considered due to their high vertical deviation from the relation between the magnitude residuals of the I-band P-L relation and the corresponding residual of the P-W relation. These deviations are possibly due to errors in the individual adopted extinctions. Since intrinsic color uncertainties are dominated by reddening uncertainties, as a final cleaning process, we did not consider Cepheids with reddening errors greater than the 95th percentile of the reddening error distribution. Consequently, 109 F Cepheids and 73 1O Cepheids were discarded.

Distances to the stars, used to calculate their I-band absolute magnitudes, were computed using the method described in Jacyszyn-Dobrzeniecka et al. (2016). We adopted their P-L relations for the full sample of F and 1O LMC Cepheids, specifically, we did not consider their P-L relation with a break. Furthermore, we considered the recent determination of the geometrical distance to the LMC by Pietrzyński et al. (2019).

3. Instability Strip borders

The intrinsic width of the IS must be corrected for any effect that could change it, to be able to compare the strip with theoretical models. As we already removed from the sample all clear outliers (also those due to luminous companions) and objects with uncertain measurements, the major factor that is left is the effect of not perfectly known reddening. The non-zero uncertainties of the applied reddening values mean that the scatter of the Cepheid colors is higher and the IS width larger. The uncertainty of the photometry itself has a similar effect but to a much lesser extent. We performed the following steps to obtain an intrinsic IS that is free of this effect. We binned the complete sample, including F and 1O Cepheids, with respect to absolute magnitude in the I-band M_I. The central bins contain 233 stars, while the faintest and brightest bins contain around 100 stars. Firstly, we determine the initials blue and red edges of the IS of each bin, by locating the $1^{\rm st}$ and $99^{\rm th}$ percentile of the intrinsic color distribution, namely $B_{\rm 1st}$ and $R_{\rm 99th}$, respectively. We then generate and add random errors to the intrinsic color of each Cepheid, making the distribution of color wider. Subsequently, we count the number of stars that lie outside the initial edges, in other words, stars bluer and redder than $B_{\rm 1st}$ and $R_{\rm 99th}$, respectively. We repeated this process 10000 times and computed the median of the distribution of the number of stars outside the initial edges, namely $n_{\rm blue}$, $n_{\rm red}$.

The final blue and red IS positions of each bin, namely, $B_{\rm final}$ and $R_{\rm final}$, were obtained by moving the initial edges "inside" the IS by $n_{\rm blue}$ and $n_{\rm red}$ stars, respectively. In this way, we subtract the widening effect due to reddening uncertainties and obtain a better approximation to the intrinsic IS. Note that only such corrected IS can be compared directly with theoretical models that are not affected by reddening. The interior and exterior uncertainties in the intrinsic color of the IS were obtained by moving $B_{\rm 1st}$ and $R_{\rm 99th}$ by the $16^{\rm th}$ and $84^{\rm th}$ percentile of the distribution of the number of stars that lie outside these initial edges. The positions in M_I of each bin of the IS edges were considered as the median of the M_I distribution of each bin. The computed IS boundaries for the complete sample are shown in Fig. 1. In this figure, the periods of the 1O Cepheids were fundamentalized using equation 1 of Pilecki et al. (2021). To obtain the overplotted constant period lines for 1, 3, and 10 days we used the period-luminosity-color

https://doi.org/10.1017/S1743921323002673 Published online by Cambridge University Press

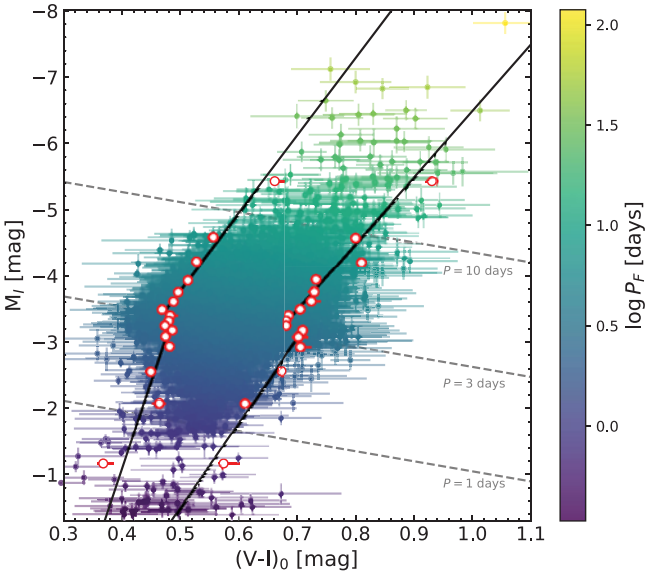

Figure 1. CMD of F and 1O LMC Cepheids. The boundaries of our empirical IS are shown as red points. Fits for the upper and lower part of the red and blue edges are shown as black solid lines. Periods for these stars are shown with a color gradient. For 1O Cepheids, periods were fundamentalized. Dashed lines of constant periods are overplotted.

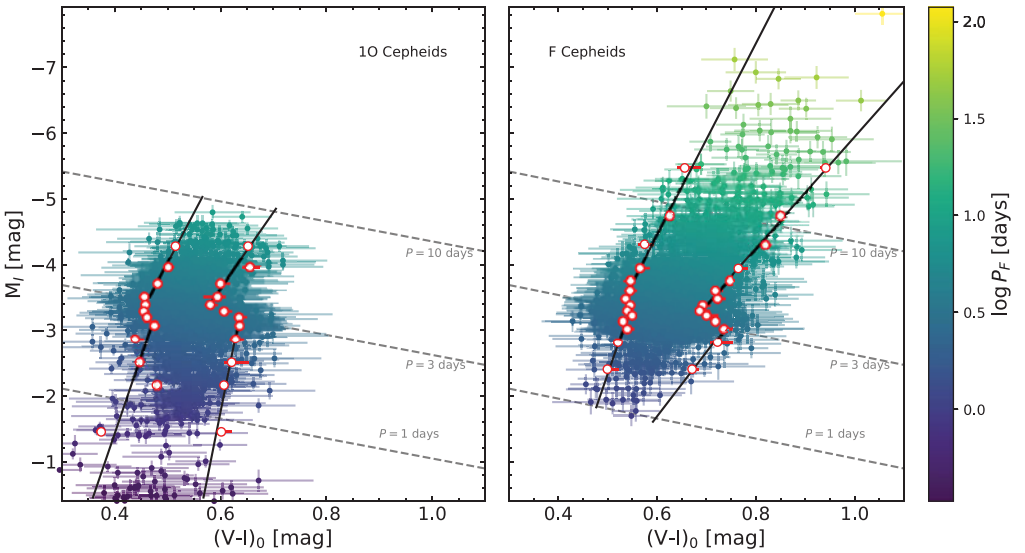

Figure 2. Same as Fig. 1, for 1O (left panel) and F (right panel) independently.

(PLC) relation computed using the previously calculated I-band absolute magnitude and intrinsic color, and the periods provided in the OGLE catalog. We repeated the IS edge determination process for F and 1O Cepheids separately, using bins that contain 162 and 109 stars, respectively. The obtained IS edges are shown in Fig. 2.

https://doi.org/10.1017/S1743921323002673 Published online by Cambridge University Press

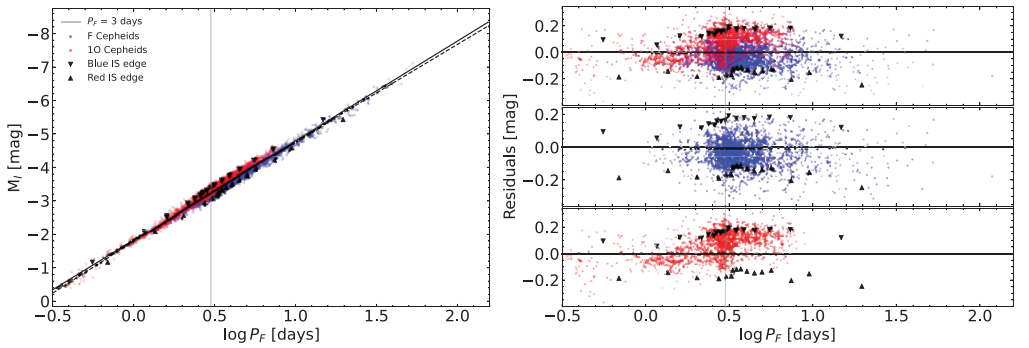

Figure 3. P-L relation of F (blue points) and 1O (red points) LMC Cepheids (left panel). The 1O Cepheid periods were fundamentalized. The boundaries of the IS are displayed as black points. At $P = 2.5$ days, a vertical gray line is traced. An average fit of the P-L relation considering the entire sample of stars is shown as a solid line. The differences between the fit of P-L and the data are presented in the right panel, for the entire sample (upper subpanel), only F Cepheids (middle subpanel), and only 1O Cepheids (lower subpanel).

4. Discussion

4.1. *Break in IS boundaries in* $(V - I)$ *color*

Previously in the literature, breaks in the P-L relation of F and 1O Cepheis have been reported in Magellanic clouds. Bauer et al. (1999); Sharpee et al. (2002) and Sandage et al. (2009) found a slope change of the P-L relation for the SMC F Cepheids with periods shorter than 2 days. On the other hand, Sandage et al. (2004) and Ripepi et al. (2022) describe a break in the PL relation for LMC Cepheids with periods of $P_F = 10$ d and $P_{1O} = 0.58$ d (the equivalent of $P_F = 0.81$ d), respectively. Bhardwaj et al. (2016, and references therein) performed an analysis of possible non-linearities in the P-L relations of Cepheids in the Magellanic clouds, confirming the statistical significance of the aforementioned breaks.

Bauer et al. (1999) proposed several possible scenarios to explain the break of the P-L relation at 2 days for the SMC. One of these scenarios, also mentioned by Ripepi et al. (2022), is the depopulation of second and third-crossing Cepheids in the faint part of the IS, due to the fact that the extension of the blue loops decreases as the mass and period of Cepheids decrease, hence these stars would spend less time inside the IS, or they would not enter at all. This implies that Cepheids fainter than the break are likely on their first crossing of the IS. This scenario should be noticeable in the CMD and could have an impact on the shape of the IS.

By analyzing the obtained IS edges of the entire sample, shown in Fig. 1, we observe that there is a break in the position of the IS boundaries, characterized by a shift to hotter temperatures above $P \sim 3$ days. This effect is also present in the IS edges of the F and 1O Cepheids subsamples (most noticeable in the red edge) presented in Fig. 2. Motivated by the detection of these breaks, using the Python package `emcee`, we performed a linear fit with two parts for our empirical IS borders. This separation considers the change of slope and discontinuity in the boundaries of the IS, between faint and bright Cepheids. In addition, a simplified wedge-shaped IS version was also computed.

In Fig. 3 we show an average P-L relation of our complete sample (considering F and 1O Cepheids), the periods of the 1O Cepheids were fundamentalized. Using the PLC relation we converted our IS to the period-luminosity plane and marked its edges with black triangles. In the right panel, we show residuals from the subtraction of the fit of the P-L relation from the data. For periods longer than $P \sim 3$ days, there is a sudden increase

https://doi.org/10.1017/S1743921323002673 Published online by Cambridge University Press

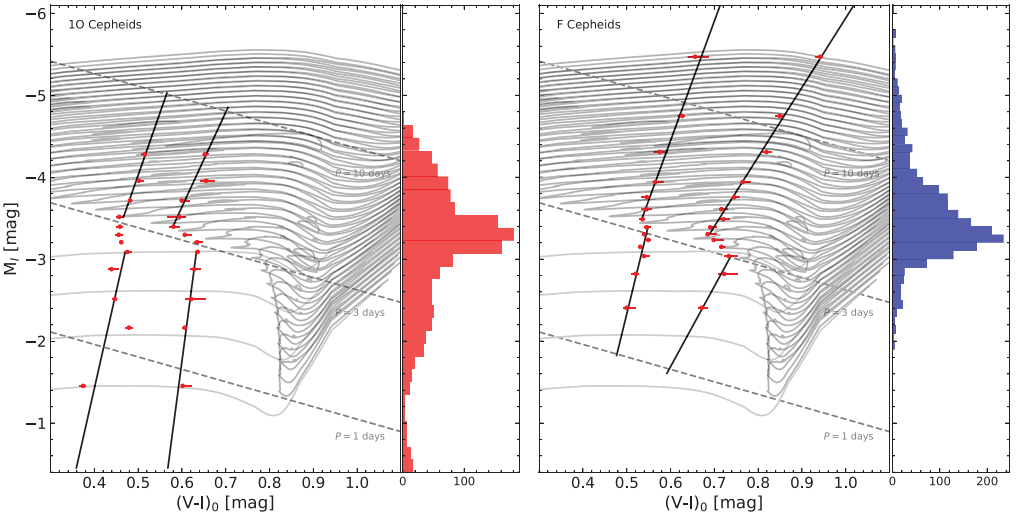

Figure 4. CMD showing the empirical IS limits (red points), separately for 1O (left panel) and F-mode (right panel) LMC Cepheids. Fits for the blue and red edge, considering a break at $P \sim 3$ days, are shown as solid blue and red lines. Blue loops of evolutionary tracks of 3 to 7 $M_\odot$ in steps of 0.1 $M_\odot$ are presented as gray lines. The subgiant phase is displayed for tracks of 3 to 4.5 $M_\odot$ in steps of 0.5 $M_\odot$. The I-band absolute magnitude distributions of the 1O and F LMC Cepheids are shown on the right side of each panel.

in the number of Cepheids. Stars with periods shorter than 2.5 days or longer than about 10 days tend to lay mostly below the P-L relation. The 10-day limit corresponds to the break reported in the literature, while below 0.81 days (a break from Ripepi et al.) we can only see another significant decrease in the number of Cepheids. Regarding the IS edges, some change can be seen at these two period values but the statistics are too low to quantify it reliably.

From a theoretical point of view, blue loops are very sensitive to metallicity and the adopted input physics, such as convective core overshooting and nuclear reactions (Xu & Li 2004a,b; Walmswell et al. 2015). Several previous works in the literature have shown that the general trend for the blue loop extension is to decrease with stellar mass. In particular, for stars with $M < 4\ M_\odot$ loops do not enter the IS (see, e.g., Anderson et al. 2016; De Somma et al. 2022). This supports the scenario proposed by Bauer et al. (1999) and Ripepi et al. (2022). To further test theoretical models and the depopulation of the faint part of the IS, using the stellar evolution code Modules for Experiments in Stellar Astrophysics (MESA; Paxton et al. 2011), we obtained evolutionary tracks for non-rotating stars covering the mass range from 3 to $7M_\odot$ in steps of $0.1M_\odot$, with metallicity $Z = 0.008$, and compared them with our IS positions. These tracks consider exponential overshooting, semi-convection, and mass loss. The comparison between the evolutionary tracks and our empirical IS borders is shown in Fig. 4. Evolutionary tracks with $M \lesssim 4.2M_\odot$ show blue loops that do not pass through the red edge of the IS. As a consequence, in this mass range, we expect an increasingly (toward shorter P) large contribution of Cepheids at the first crossing through the IS, where they evolve in a short time scale of the H-shell burning phase. Such first-crossing Cepheids spend less time within the IS compared to higher mass Cepheids, thus it is expected to find fewer stars in this part of the IS. On the other hand, evolutionary tracks with $M \gtrsim 4.2M_\odot$ present blue loops that cross the red edge of the IS, therefore the fraction of Cepheids in the second and third crossings, evolving in the longer time scale of the He-core burning

https://doi.org/10.1017/S1743921323002673 Published online by Cambridge University Press

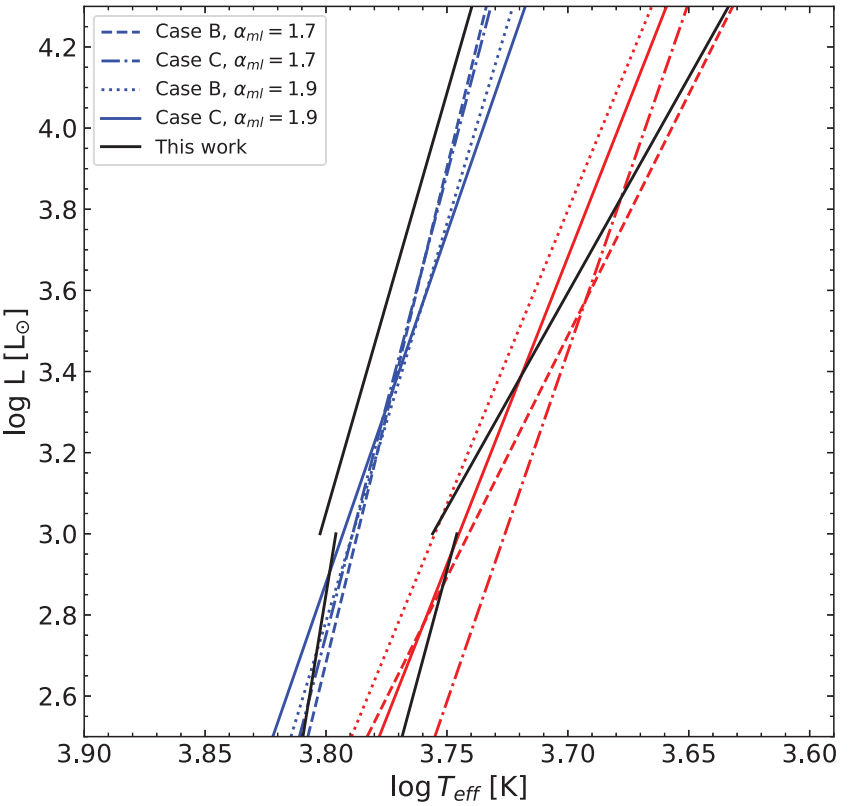

Figure 5. Comparison of theoretical ISs presented in De Somma et al. (2022) (blue and red) and our empirical IS (black) in an HRD. Different line styles represent different cases of increase in the luminosity, over their canonical model and efficiencies of superadiabatic convection α_{ml}.

phase, increases considerably. Since these stars spend more time inside the strip, their total number is much larger than the stars in the lower part of the IS.

4.2. *Comparison with theoretical ISs*

Previous works in the literature have obtained theoretical IS edges and have studied the effects of, for example, rotation, metallicity, and overshooting. By comparing these theoretical results with our empirical IS, it is possible to constrain some of the physical effects studied. Each point of our IS for F Cepheids in the CMD plane was converted to the $\log T_{\rm eff} - \log L$ plane using the color-temperature and bolometric correction calibration presented by Worthey & chul Lee (2011). Then the points were fitted in the same way as for the IS in the color-magnitude diagram. Since our empirical edges are composed of two parts, the conclusions may be different for the lower and upper parts of the IS.

In Fig. 5, we show the theoretical ISs obtained by De Somma et al. (2022). Their models are based on Bag of Stellar Tracks and Isochrones (BaSTI; Hidalgo et al. 2018) evolutionary tracks that take into account core overshooting and mass loss, and were calculated for a metallicity $Z = 0.008$. As far as their pulsation calculations go, De Somma et al. (2022) approximate the effects of overshooting by considering an increase in the luminosity, over their canonical models, of $\Delta(\log L/L_\odot) = 0.2$ dex (case B), and $\Delta(\log L/L_\odot) = 0.4$ dex (case C), considering in addition 2 values for the superadiabatic convection efficiency, $\alpha_{ml} = 1.7$ and $\alpha_{ml} = 1.9$. Globally, our empirical edges are most consistent with their

https://doi.org/10.1017/S1743921323002673 Published online by Cambridge University Press

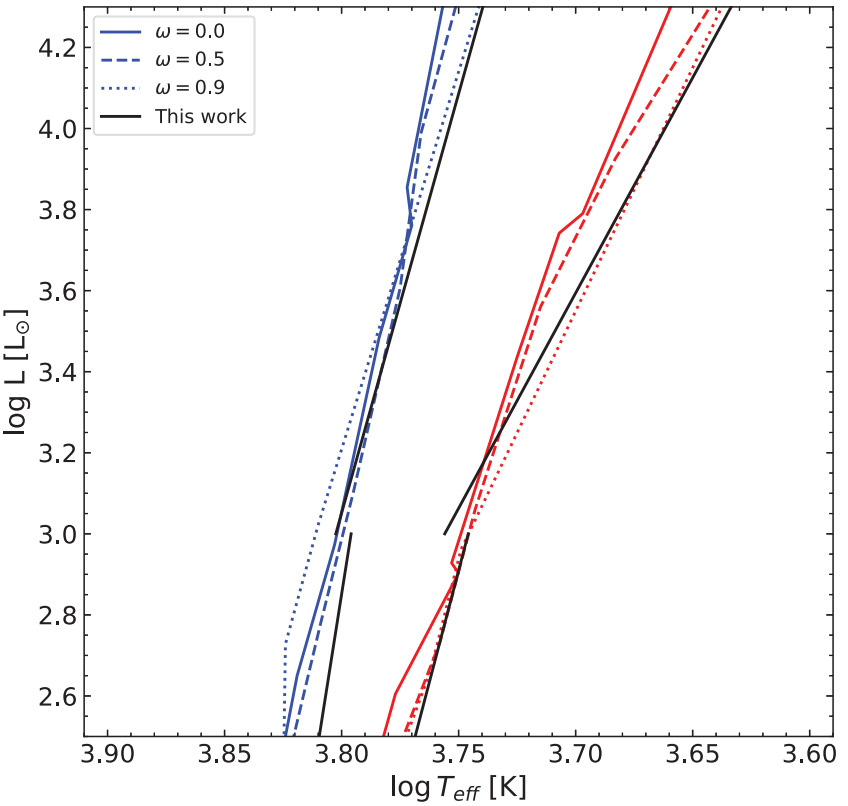

Figure 6. Comparison of theoretical ISs presented in Anderson et al. (2016) (blue and red) and our empirical IS (black) in a HRD. Different line styles represent different rotation rates ω.

models for case B and $\alpha_{\rm ml} = 1.7$. However, there are some noticeable differences – our upper blue edge is systematically hotter, and although the other edges coincide better with the theoretical ones, their slopes are slightly different.

The theoretical instability strips of Anderson et al. (2016) are shown in Fig. 6. They use the Geneva code of stellar evolution (Eggenberger et al. 2008), varying metallicity, and rate of rotation. We compare our results with their ISs for $Z = 0.006$, and three rotation rates $\omega = 0.0$, 0.5, and 0.9. Their edges agree remarkably well with our empirical edges, both in regard to the zero points and the slopes, with only our blue edge being systematically cooler. Globally their models with high rotation rates describe best our determined edges but the lower part seems to favor slightly better those with moderate rotation rates.

Paxton et al. (2019) introduce Radial Stellar Pulsation `RSP`, a functionality in the MESA code to model high-amplitude, self-excited, non-linear pulsations that the star develops when it crosses the IS. The `RSP` model depends on equations describing time-dependent convection, described in Smolec & Moskalik (2008), which also depend on free parameters. Pulsation periods depend weakly on these parameters. However, period growth rates and light curves are sensitive to the choice of these convective variables. Different sets for these parameters are shown in table 4 of Paxton et al. (2019). In Fig. 7, the theoretical ISs borders presented by Paxton et al. (2019, priv. communication) considering set B and D, for $Z = 0.008$ are shown. Their ISs were computed using second and third crossing Cepheid models. Set B of convective parameters adds radiative cooling effects to the convective model, while the parameter set D simultaneously includes

https://doi.org/10.1017/S1743921323002673 Published online by Cambridge University Press

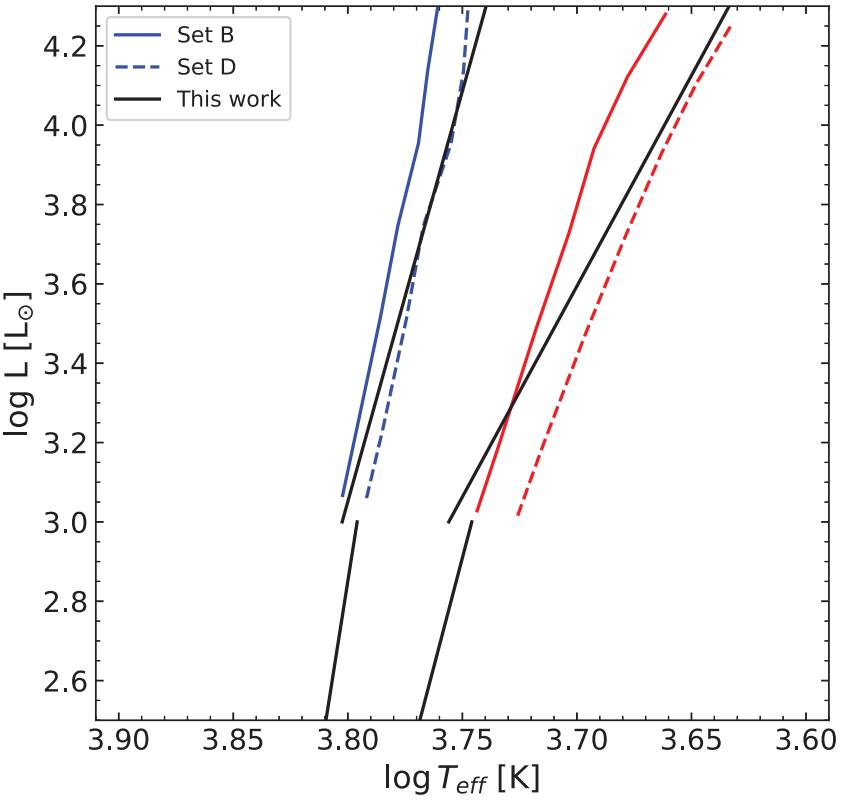

Figure 7. Comparison of theoretical ISs presented in Paxton et al. (2019) (blue and red) and our empirical IS (black) in an HRD. Different line styles represent different sets of convective parameters of RSP.

the effects of turbulent pressure and turbulent flow in addition to radiative cooling. As mentioned in Paxton et al. (2019), the IS edges produced by sets A and C overlap those for convective sets B and D, respectively. We can see that our blue edge is in closer agreement with that of set D, while our red edge lies somewhere in between sets B and D. The red edge is actually described better by set D for luminous long-period Cepheids, and by set B for short-period Cepheids, also if we extrapolate their red edge down to fainter Cepheids.

5. Conclusions

We used a sample of LMC Cepheids from the OGLE-IV catalog to compute the empirical, intrinsic instability strip. We determined the IS edges for F and 1O Cepheids, together and separately, using $V-$ and I-bands. In all cases, a break in the IS was observed at $\log P \sim 3$ days, which is most noticeable in the red edges and for separate 1O and F samples.

Using a set of evolutionary tracks computed with the stellar evolution code MESA, we investigated the scenario in which the origin of this break is explained by depopulation in the faint part of the IS. Such depopulation would be caused by too low an extension of blue loops for lower-mass stars, which would not evolve blueward enough to enter the instability strip. Our results confirmed the conclusions from other studies in the literature on that subject (Bauer et al. 1999; Ripepi et al. 2022).

https://doi.org/10.1017/S1743921323002673 Published online by Cambridge University Press

Consequently, Cepheids with masses below $\sim 4M_{\odot}$ would be found mostly during the first crossing of the IS, while above this limit there is a much higher contribution of Cepheids at the second and third crossing, for which the time scales are much longer. This change from the domination of the first to the domination of subsequent crossings coincides with the observed break in the IS edges. At the same time at different crossings, we may expect slightly different pulsational properties as the Cepheids are found at different evolutionary stages, i.e. the subgiant and blue loop phases of evolution. These two populations of Cepheids with different properties dominating at a given mass (or period) range, may then affect the position of the IS edges.

We compared our results with theoretical instability strips published in the literature. Our empirical edges are best described by the models of Anderson et al. (2016) with high rotation rates, for periods above the break, and by models with moderate rotation rates below the break. However, regarding the red edge only, models with $\omega = 0.9$ describe well the whole range of pulsation periods.

Regarding the instability strips that result from the models of De Somma et al. (2022) and Paxton et al. (2019), some fine-tuning of parameters would be needed to obtain consistent results. At the moment, no single set of their parameters produces an IS that would correspond well with our empirical edges – they either fall between the different sets or have different slopes. Such fine-tuning is beyond the scope of this work. At the moment for that purpose, we suggest using the models of Anderson et al. (2016) with either high rotation rates or a mixture of moderate and high rotation rates depending on the pulsation period.

Putting constraints on the models, apart from finding the one that describes the observations best, at the same time we can learn about the physical properties of classical Cepheids, their pulsational properties, and the evolution of intermediate-mass stars.

References

Anderson, R. I., Saio, H., Ekström, S., Georgy, C., & Meynet, G. 2016, A&A, 591, A8
Bauer, F., Afonso, C., Albert, J. N., et al. 1999, A&A, 348, 175
Bhardwaj, A., Kanbur, S. M., Macri, L. M., et al. 2016, MNRAS, 457, 1644
Bono, G., Caputo, F., Cassisi, S., et al. 2000a, ApJ, 543, 955
Bono, G., Castellani, V., & Marconi, M. 2000b, ApJ, 529, 293
Caldwell, J. A. R. & Laney, C. D. 1991, in The Magellanic Clouds, ed. R. Haynes & D. Milne, Vol. 148, 249
Chen, B. Q., Guo, H. L., Gao, J., et al. 2022, MNRAS, 511, 1317
De Somma, G., Marconi, M., Molinaro, R., et al. 2022, ApJs, 262, 25
Eggenberger, P., Meynet, G., Maeder, A., et al. 2008, Ap&SS, 316, 43
Fernie, J. D. 1990, ApJ, 354, 295
Fiorentino, G., Caputo, F., Marconi, M., & Musella, I. 2002, ApJ, 576, 402
Fiorentino, G., Marconi, M., Musella, I., & Caputo, F. 2007, A&A, 476, 863
Górski, M., Zgirski, B., Pietrzyński, G., et al. 2020, ApJ, 889, 179
Hidalgo, S. L., Pietrinferni, A., Cassisi, S., et al. 2018, ApJ, 856, 125
Inno, L., Bono, G., Matsunaga, N., et al. 2016, ApJ, 832, 176
Jacyszyn-Dobrzeniecka, A. M., Skowron, D. M., Mróz, P., et al. 2016, Acta Astron.,, 66, 149
Madore, B. F., Freedman, W. L., & Moak, S. 2017, ApJ, 842, 42
Martin, W. L., Warren, P. R., & Feast, M. W. 1979, MNRAS, 188, 139
Musella, I. 2022, Universe, 8, 335
Narloch, W., Pietrzyński, G., Kołaczkowski, Z., et al. 2019, MNRAS, 489, 3285
Paxton, B., Bildsten, L., Dotter, A., et al. 2011, ApJs, 192, 3
Paxton, B., Smolec, R., Schwab, J., et al. 2019, ApJs, 243, 10
Pel, J. W. & Lub, J. 1978, in The HR Diagram - The 100th Anniversary of Henry Norris Russell, ed. A. G. D. Philip & D. S. Hayes, Vol. 80, 229

https://doi.org/10.1017/S1743921323002673 Published online by Cambridge University Press

Petroni, S., Bono, G., Marconi, M., & Stellingwerf, R. F. 2003, ApJ, 599, 522
Pietrzyński, G., Graczyk, D., Gallenne, A., et al. 2019, Nature, 567, 200
Pilecki, B. 2022, in XL Polish Astronomical Society Meeting, ed. E. Szuszkiewicz, A. Majczyna, K. Małek, M. Ratajczak, E. Niemczura, U. B"kak-St"keślicka, R. Poleski, M. Bilicki, & Ł. Wyrzykowski, Vol. 12, 174–177
Pilecki, B., Pietrzyński, G., Anderson, R. I., et al. 2021, ApJ, 910, 118
Pilecki, B., Thompson, I. B., Espinoza-Arancibia, F., et al. 2022, ApJl, 940, L48
Ripepi, V., Chemin, L., Molinaro, R., et al. 2022, MNRAS, 512, 563
Sandage, A., Tammann, G. A., & Reindl, B. 2004, A&A, 424, 43
Sandage, A., Tammann, G. A., & Reindl, B. 2009, A&A, 493, 471
Sharpee, B., Stark, M., Pritzl, B., et al. 2002, AJ, 123, 3216
Skowron, D. M., Skowron, J., Udalski, A., et al. 2021, ApJs, 252, 23
Smolec, R. & Moskalik, P. 2008, Acta Astron.,, 58, 193
Soszyński, I., Udalski, A., Szymański, M. K., et al. 2015, Acta Astron.,, 65, 297
Tammann, G. A., Sandage, A., & Reindl, B. 2003, A&A, 404, 423
Turner, D. G. 2001, Odessa Astronomical Publications, 14, 166
Ulaczyk, K., Szymański, M. K., Udalski, A., et al. 2013, Acta Astron.,, 63, 159
Walmswell, J. J., Tout, C. A., & Eldridge, J. J. 2015, MNRAS, 447, 2951
Worthey, G. & chul Lee, H. 2011, The Astrophysical Journal Supplement Series, 193, 1
Xu, H. Y. & Li, Y. 2004a, A&A, 418, 213
Xu, H. Y. & Li, Y. 2004b, A&A, 418, 225

https://doi.org/10.1017/S1743921323002673 Published online by Cambridge University Press